Accurate numerical study of the stability of Na_{19}-cluster dimers

E. Engel, U. R. Schmitt, H.-J. Lüdde, A. Toepfer, E. Wüst, and R. M. Dreizler
Institut für Theoretische Physik, Universität Frankfurt, Robert Mayer Strasse 8-10, 6000 Frankfurt/Main 11, Germany

O. Knospe and R. Schmidt
Institut für Theoretische Physik, Technische Universität Dresden, Mommsenstrasse 13, 8027 Dresden, Germany

P. Chattopadhyay
Department of Physics, Maharshi Dayanand University, Rohtak, Haryana 124001, India
(Received 16 November 1992)

We investigate the structure of $(Na_{19})_2$-cluster dimers via solution of the Kohn-Sham equations for a two-center jellium model. Results for the binding energy of the dimer as a function of the intercluster separation as well as the electronic correlation diagram of the $(Na_{19})_2$ system are presented. In contrast to previous results, our calculations indicate that the barrier which separates a local minimum in the binding energy at an intercluster separation of about 15 a.u. from the absolute minimum, the united Na_{38} cluster, is rather small.

I. INTRODUCTION

The spherical jellium model introduced by Ekardt,[1] Beck,[2] and Chou, Cleland, and Cohen[3] has been shown to explain a number of characteristic features of metal clusters, most notably the existence of magic numbers (for an overview see, e.g., Refs. 4 and 5; for work on shells and supershells in metal clusters, see Refs. 6–11). The standard spherical model can be refined further by the introduction of axial deformation[12,13] and of a finite surface thickness of the jellium background.[14] In addition to the investigation of ground state properties of metal clusters, the jellium model has been employed with success for the study of the optical response properties[15–21] and of elastic electron-cluster scattering.[22]

On the basis of the jellium model, Saito and Ohnishi[23] (referred to as SO hereafter) have discussed the formation of $(Na_{19})_2$-cluster dimers as an intermediate step in a complete fusion process of two Na_{19} clusters. They found that the dimer binding energy

$$\Delta E(d) = E_{\rm tot}(d) - E_{\rm tot}(\infty) \quad , \tag{1}$$

where $E_{\rm tot}(d)$ is the total energy of the dimer $(Na_{19})_2$ for a given intercluster separation d and $E_{\rm tot}(\infty)$ is the total energy of two separated, spherical Na_{19} clusters, has an attractive local minimum at $d \approx 16$ a.u., which is separated from the absolute minimum at $d = 0$, representing the united Na_{38} cluster, by a substantial barrier. SO interpreted the system at this local minimum as a "giant atom dimer," in close analogy to atomic alkali dimers such as Na_2. Given the high abundance of Na_{19} clusters in experimental mass spectra,[24] the reactivity of Na_{19} clusters and the stability of $(Na_{19})_2$ dimers were suggested to induce fusion of two Na_{19} clusters and thus to explain the relatively high abundance of Na_{38} clusters in the mass spectra, which cannot be understood in terms of the spherical jellium model. The same concept has been applied to $(Na_4)_2$ and $(Na_8)_2$ dimers by Ishii, Saito, and Ohnishi[25] and to the dimer decay of potassium clusters by Saito and Cohen.[26] Furthermore, Nakamura *et al.*[27] used a similar approach for the discussion of cluster fragmentation. Recently, relatively stable cluster molecules have also been found in quantum molecular-dynamics simulations of Na_9-Na_9 and Na_8-Na_8 collisions.[28]

In the present study we reanalyze the problem considered by SO. Our approach is thus similar to that of these authors, that is, we solve the Kohn-Sham equations for the valence electrons in the local-density approximation (LDA) for a two-center jellium model. As the results obtained depend rather sensitively on the accuracy of the numerical procedures used, we put special emphasis on this point. In addition, we investigate the dependence of the results on the specific form of the correlation contributions to total energies and Kohn-Sham potentials. In particular, we compare results obtained with the Gunnarsson-Lundqvist (GL) (Ref. 29) parametrization of the LDA correlation functional with those obtained for the form given by Vosko, Wilk, and Nusair (VWN) (Ref. 30). While for unpolarized systems the latter functional, in general, leads to results rather similar to those from the Perdew-Zunger (PZ) form[31] (without self-interaction correction) used by SO and seems to be among the most accurate representations of the electron-gas correlation energy available today, the GL functional produces a somewhat larger correlation energy.[30,31] This effect also shows up in jellium model calculations. Nonetheless, the variation of the binding energy $\Delta E(d)$ with the intercluster separation is quite similar for the GL and VWN functionals. One obtains a local minimum for an intercluster separation of about 15 a.u. The barrier separating this minimum from the united cluster is, on the other hand, much smaller in height and width than the barrier reported by SO.

Further insight into the numerical accuracy as well as the structure of the binding energy can be obtained from the electron correlation diagram, that is, the variation of the self-consistent Kohn-Sham orbital energies with the intercluster separation.[32,33] Correlation diagrams have provided a very valuable guide for the study of excitation and electron transfer processes in ion-atom collisions at moderate collision energies. They can be expected to be of equal use for the discussion of atom-cluster or, to refer to our specific example, of cluster-cluster collisions at sufficiently low energies.

The paper is organized as follows: In Sec. II we outline the theoretical framework. Section III explains the numerical procedures used and discusses the characteristics and limitations of our method. In Sec. IV our results for the $(Na_{19})_2$ dimer are given. An Appendix summarizes some details concerning the background potential for the case of overlapping jellium spheres. We use atomic units throughout this paper unless otherwise stated.

II. THEORY

In the spherical jellium model one assumes that the ionic cores in the cluster are well described by a positive charge distributed uniformly over a sphere with radius

$$R = r_S N^{\frac{1}{3}} \quad . \tag{2}$$

Here r_S denotes the Wigner-Seitz radius of the bulk metal ($r_S = 3.93$ for Na) and N is the number of atoms in the cluster. The valence electrons are then bound by the electrostatic potential generated by this background charge. In the present situation the two separated Na_{19} clusters are described by jellium spheres, whose centers are a distance $d = 2f$ apart. For the case of overlapping clusters ($f < R_{Na_{19}} = 10.487$ a.u.), we require the background charge density to be homogeneous and equal to the bulk value $n_0 = (\frac{4\pi}{3} r_S^3)^{-1}$ inside the two overlapping spheres. This is assured by adjusting the radius of the truncated spheres, so that in cylindrical coordinates (ρ, φ, z) one has

$$n_+(\mathbf{r}) = n_0 \Theta(R_d^2 - \rho^2 - (|z| - f)^2) \quad , \tag{3}$$

where $\Theta(x)$ represents the usual step function, i.e., $\Theta(x) = 1$ for $x > 0$ and 0 otherwise, and the modified radius R_d of the truncated spheres is directly obtained from the radius R of the corresponding isolated spheres, Eq. (2), using the Cardanic formula,

$$R_d = R\left[B + \frac{f^2}{4BR^2} - \frac{f}{2R}\right],$$

$$B = \left[1 + \frac{f^3}{8R^3} + \sqrt{1 + \frac{f^3}{4R^3}}\right]^{\frac{1}{3}} \quad .$$

The electrostatic potential corresponding to this background charge density, denoted by $v_{\text{ext}}(\mathbf{r})$, is most easily evaluated by a multipole expansion (for details see the Appendix).

For the solution of the many-body problem at hand, we work within the framework of density-functional theory (DFT), which has also been the basis for extensive work on atomic dimers (and more complicated molecules — for references see, e.g. Ref. 34). In order to reduce the numerical task somewhat, we restricted ourselves to the spin-saturated case. As SO clearly demonstrate, the spin polarized results are rather close to the unpolarized ones, the latter representing the ground state in the most interesting region of distances f. The maximum difference between both spin versions occurs for the united cluster. One may obtain an idea of the energy differences involved by analyzing the spherically averaged Na_{38} ground state for both situations: While the spin-polarized case leads to a ground-state energy of $-2.665\,73$ a.u. (using VWN), the unpolarized version gives $-2.662\,62$ a.u. The difference of $0.003\,11$ a.u. is much smaller than the energy difference with respect to two single Na_{19} clusters, $\Delta E(f = 0) = -0.041\,42$ a.u. Consequently, even for such f where the spin-polarized case represents the true ground state, the $\Delta E(f)$ resulting from an unpolarized calculation is close to the correct spin-polarized $\Delta E(f)$ (compare Fig. 1 of SO).

Within DFT one has to solve the Kohn-Sham equations (for each separation f),

$$\left(-\frac{\triangle}{2} + v_{\text{KS}}([n];\mathbf{r})\right)\Psi_\alpha(\mathbf{r}) = \epsilon_\alpha \Psi_\alpha(\mathbf{r}) \quad , \tag{4}$$

where the total potential $v_{\text{KS}}([n];\mathbf{r})$ is given by

$$v_{\text{KS}}([n];\mathbf{r}) = v_{\text{ext}}(\mathbf{r}) + v_H(\mathbf{r}) + v_{\text{xc}}([n];\mathbf{r}) \quad . \tag{5}$$

Here v_{ext} is the background potential (its form for the case of overlapping jellium spheres is discussed in the Appendix), v_H is the Hartree potential,

$$v_H(\mathbf{r}) = \int d^3r' \frac{n(\mathbf{r}')}{|\mathbf{r} - \mathbf{r}'|}, \tag{6}$$

and v_{xc} is the exchange-correlation potential, defined as the functional derivative of the exchange-correlation energy functional $E_{\text{xc}}[n]$,

$$v_{\text{xc}}([n];\mathbf{r}) \equiv \frac{\delta E_{\text{xc}}[n]}{\delta n(\mathbf{r})} \quad . \tag{7}$$

In our calculations $E_{\text{xc}}[n]$ has been taken into account in the LDA. We carried through all our calculations for two different versions of $E_{xc}^{\text{LDA}}[n]$, the form suggested by Gunnarsson and Lundqvist[29] and the interpolation between the RPA (being exact in the high density limit) and accurate low-density Monte Carlo results[35] by Vosko, Wilk, and Nusair,[30] in order to demonstrate that our main conclusions are not due to a specific form of $E_{\text{xc}}^{\text{LDA}}[n]$. Equation (4) has to be solved self-consistently with the ground-state density n constructed from the N lowest occupied orbitals Ψ_α.

For the solution of the two-center Kohn-Sham equations (4), we use prolate spheroidal coordinates ξ, η, φ, which have been utilized for related problems by various authors (see, e.g., Refs. 32, 33, 13). While ξ and η are defined in terms of the distances r_1 and r_2 from the two jellium centers to the point $\mathbf{r}$ by

$$\xi = \frac{(r_1 + r_2)}{2f}, \qquad 1 \le \xi < \infty \tag{8}$$

$$\eta = \frac{(r_1 - r_2)}{2f}, \qquad -1 \le \eta \le 1 \tag{9}$$

φ is the usual azimuthal angle, $0 \le \varphi \le 2\pi$, with respect to the intercenter axis. Due to the rotational symmetry with respect to the intercenter axis,

$$v_{\rm KS}(\mathbf{r}) = v_{\rm KS}(\xi,\eta) \quad ,$$

the solutions of (4) can be classified by the angular-momentum projection quantum number m, and one can decompose the eigenstates as

$$\Psi_\alpha(\mathbf{r}) = \Psi_{j,m}(\xi,\eta)e^{\pm im\varphi} \quad , \quad m = 0,1,2,\ldots \quad . \tag{10}$$

The integer $j = 1,2,\ldots$ denotes the sequence of levels for given m. Consequently the Kohn-Sham equations to be solved read

$$\{t_{\xi\eta} + v_{\rm KS}(\xi,\eta)\}\Psi_{j,m}(\xi,\eta) = \epsilon_{jm}\Psi_{j,m}(\xi,\eta), \tag{11}$$

with

$$t_{\xi\eta} = \frac{-1}{2f^2(\xi^2-\eta^2)}\left[\partial_\xi(\xi^2-1)\partial_\xi + \partial_\eta(1-\eta^2)\partial_\eta - \frac{(\xi^2-\eta^2)m^2}{(\xi^2-1)(1-\eta^2)}\right] \quad .$$

For such a two-dimensional problem it seems advantageous[32,33,23,13,26] to expand $\Psi_{j,m}(\xi,\eta)$ in terms of analytical basis functions ψ_{nlm},

$$\Psi_{j,m}(\xi,\eta) = \sum_{n=0,l=m}^{\infty} f^j_{nlm}\psi_{nlm}(\xi,\eta) \quad . \tag{12}$$

Here we use the nonorthogonal Hylleraas basis,[36,32,33]

$$\psi_{nlm}(\xi,\eta) = (\xi^2-1)^{\frac{m}{2}}e^{-\frac{\xi-1}{2a}}L^m_n\left(\frac{\xi-1}{a}\right)P^m_l(\eta) \ , \tag{13}$$

where the L^m_n and P^m_l are the generalized Laguerre polynomials and the associated Legendre functions, respectively, and a is an adjustable basis parameter (for a discussion of a, see Sec. III). With this basis, Eq. (11) can be recast as an algebraic eigenvalue problem,

$$\sum_{n'=0}^{n_{\max}}\sum_{l'=m}^{m+l_{\max}}[\langle nlm|t_{\xi\eta} + v_{\rm KS}|n'l'm\rangle - \epsilon_{jm}\langle nlm|n'l'm\rangle]f^j_{n'l'm} = 0, \tag{14}$$

where m=0,1,...,$m_{\max}$ and $\langle\xi,\eta|nlm\rangle \equiv \psi_{nlm}(\xi,\eta)$. Also, we have indicated that for any calculation, the basis expansion has to be truncated. While the overlap and kinetic matrix elements $\langle nlm|n'l'm\rangle$ and $\langle nlm|t_{\xi\eta}|n'l'm\rangle$, respectively, can be evaluated analytically,[32] the potential matrix elements

$$\langle nlm|v_{\rm KS}|n'l'm\rangle = f^3\int_1^\infty d\xi\int_{-1}^1 d\eta(\xi^2-\eta^2)\psi_{nlm}(\xi,\eta)\times v_{\rm KS}(\xi,\eta)\psi_{n'l'm}(\xi,\eta) \tag{15}$$

have to be treated numerically.

Equation (14) has to be solved self-consistently, i.e., $v_{\rm KS}$ is obtained from Eq. (5) using the electronic density

$$n(\xi,\eta) = \sum_{m=0}^{\infty}\sum_{j=1}^{\infty}\Theta(\varepsilon_F - \epsilon_{jm})\nu_m|\Psi_{j,m}(\xi,\eta)|^2 \quad , \tag{16}$$

where ε_F is the Fermi energy and ν_m accounts for the degeneracy for given $m = |m|$,

$$\nu_m = \begin{cases} 2 & \text{for } m = 0 \\ 4 & \text{for } m > 0. \end{cases} \tag{17}$$

Finally, the total energy was evaluated from the relation

$$E_{\rm tot} = \sum_{m=0}^{\infty}\sum_{j=1}^{\infty}\Theta(\varepsilon_F - \epsilon_{j,m})\nu_m\epsilon_{jm} + E_{\rm xc} + E_{\rm jelli} - \pi f^3\int_1^\infty d\xi\int_{-1}^1 d\eta(\xi^2-\eta^2)n(\xi,\eta)v_H(\xi,\eta) - 2\pi f^3\int_1^\infty d\xi\int_{-1}^1 d\eta(\xi^2-\eta^2)n(\xi,\eta)v_{\rm xc}(\xi,\eta) \quad , \tag{18}$$

where $E_{\rm xc}$ is the exchange-correlation energy obtained by insertion of the density (16) into the functionals of Refs. 29 and 30 and $E_{\rm jelli}$ is the electrostatic energy of the homogeneous background.

III. DETAILS OF THE NUMERICAL PROCEDURES

In this section we discuss a number of technical details of our calculations with specific emphasis on the accuracy and limitations of our method. Instead of applying the direct integration indicated in Eq. (6), it is more convenient to evaluate v_H by solution of the Poisson equation. Utilizing a multipole expansion,

$$v_H(\xi,\eta) = \frac{1}{2}\sum_{l=0}^{l_{\max}}(2l+1)\chi_l(\xi)P_l(\eta) \quad , \tag{19}$$

one ends up with differential equations for the functions χ_l,

$$\{\partial_\xi(\xi^2-1)\partial_\xi - l(l+1)\}\chi_l(\xi) = -4\pi f^2\int_{-1}^1 d\eta(\xi^2-\eta^2)P_l(\eta)n(\xi,\eta) \quad , \tag{20}$$

which have been solved by a standard shooting procedure. Several tests showed that the maximum l in this expansion can be chosen to be identical to the maximum l in the basis expansion, Eq. (14) (or somewhat smaller for small f). As boundary conditions we used

$$\left(\partial_\xi - \frac{l(l+1)}{2}\right)\chi_l(\xi)\Big|_{\xi=1} = -2\pi f^2\int_{-1}^1 d\eta(1-\eta^2)P_l(\eta)n(1,\eta) \tag{21}$$

at the lower end of the ξ interval. In the asymptotic

regime, i.e., for large ξ, the right-hand side of Eq. (20) vanishes exponentially due to the exponential decay of the density. Thus, up to exponentially decaying correction terms, the χ_l asymptotically are proportional to the Legendre functions of the second kind, $Q_l(\xi)$,[37]

$$\chi_l(\xi) \underset{\xi\gg 1}{=} c_l Q_l(\xi) \quad , \tag{22}$$

as these satisfy the proper boundary conditions,

$$\chi_l(\xi) \underset{\xi\to\infty}{\longrightarrow} 0 \quad .$$

The multipole coefficients c_l can be evaluated by multiplying Eq. (20) by $P_l(\xi)$ and integrating over ξ,

$$c_l = 4\pi f^2 \int_1^\infty d\xi \int_{-1}^1 d\eta (\xi^2-\eta^2) P_l(\xi) P_l(\eta) n(\xi,\eta) \quad . \tag{23}$$

Thus c_0 is obtained directly as

$$c_0 = 2\frac{N}{f},$$

such that the asymptotic boundary condition for the monopole term reads

$$\chi_0(\xi_{\max}) = \frac{N}{f} \ln\left|\frac{\xi_{\max}+1}{\xi_{\max}-1}\right| \quad , \tag{24}$$

with $\xi_{\max}$ being the maximum ξ value of the mesh used. The explicit calculation of higher multipole coefficients can be avoided by using the boundary conditions

$$\left.\frac{\partial_\xi \chi_l(\xi)}{\chi_l(\xi)}\right|_{\xi=\xi_{\max}} = \left.\frac{\partial_\xi Q_l(\xi)}{Q_l(\xi)}\right|_{\xi=\xi_{\max}} \quad . \tag{25}$$

For the shooting procedure we required an absolute accuracy of 10^{-8} a.u. for the $\chi_l(\xi)$. To achieve this accuracy for the higher multipoles, the mesh for this procedure was chosen independently of the Gaussian mesh used for numerical integration (see below). Thus to obtain the inhomogeneous term of Eq. (20) on the shooting mesh and the $\chi_l(\xi)$ on the Gaussian mesh, we had to use a spline interpolation.

For the numerical evaluation of the matrix elements (15) and the total energy (18), we used a two-dimensional Gaussian integration with up to 256 mesh points for each coordinate. It is noteworthy to mention that even these rather large Gaussian meshes covering the complete space inside and outside the jellium are not sufficient to obtain E_{jelli} with the required accuracy due to the sharp jellium edge (the error being of the order of 0.1 a.u.). Thus E_{jelli} has been calculated on Gaussian meshes with mesh points only inside the jellium, i.e., taking into account the jellium geometry. Alternatively, one could evaluate E_{jelli} analytically using the multipole expansion of Ref. 38. For all other quantities to be integrated, a comparison with results based on half as many mesh points showed that the integration had converged.

Also, the size of our basis has been tested extensively. It turned out that $n_{\max}=12$ and $l_{\max}=12$ are sufficient for most f. For very small f, however, we had to increase $n_{\max}$, while $l_{\max}$ could be chosen smaller than 12 (for $f=0.25$ a.u. we used $n_{\max}=18$, $l_{\max}=10$). $m_{\max}$, on the other hand, depends on f: While for $f>5$ a.u. only $m=0,1,2$ states are among the occupied orbitals, for smaller f, also the lowest $m=3$ state is occupied.

The coupled solution of Eqs. (14) and (19) proceeded iteratively, requiring the maximum absolute difference between the total potentials of two successive iterations to be smaller than 10^{-4} a.u. Solutions have been obtained in the interval 0.25 a.u. $\le f \le$ 11.5 a.u. in steps of about 0.25 a.u.

One of the crucial parameters in the basis expansion (12) is the scaling constant a. First, it determines the location of the extrema and zeros of the L_n^m. Even more important, however, is its decisive role for the asymptotic behavior of the basis functions ψ_{nlm},

$$\psi_{nlm}(\xi,\eta) \underset{\xi\gg 1}{\sim} \xi^{n+m}\, e^{-\frac{\xi}{2a}} P_l^m(\eta) \quad .$$

This has to be contrasted by the exact asymptotic form of the solutions of Eq. (11),

$$\Psi_{jm}(\xi,\eta) \underset{\xi\gg 1}{\sim} \frac{1}{\xi} e^{-f\sqrt{-2\epsilon_{jm}}\xi} \sum_{l=0}^{\infty} c_{jm}^l P_l^m(\eta) \quad .$$

At first glance one would conclude that adjusting a to some average eigenvalue $\bar{\epsilon}$, i.e., $1/a = 2f\sqrt{-2\bar{\epsilon}}$, should be a reasonable choice for a, in particular, given the fact that the eigenvalues ϵ_{jm} of a jellium calculation are rather close together. One must not underestimate, however, the importance of the power of ξ in front of the exponential term: An a smaller than this is required in order to simulate the $1/\xi$ prefactor in Ψ_{jm}. Thus we have adjusted a to be as close to $2f\sqrt{-2\bar{\epsilon}}$ as possible without producing basis functions that extend too much into the asymptotic regime.

As a is the parameter our results are most sensitive to, one can obtain an estimate of their accuracy by comparing the results for two different choices of a. For this comparison we have chosen $f=4$ a.u., as this is one of the more critical cluster-cluster separations and our results for this f deviate considerably from those of SO. Following our standard procedure for the choice of a, we find $a=0.081$ a.u. (from an average eigenvalue as discussed above, one would conclude $a\approx 0.24$ a.u.). Using the VWN functional, we obtained $\Delta E(f) = -0.0259$ a.u. Furthermore, the eigenvalue of the highest occupied orbital turned out to be $-0.098\,43$ a.u. With $a=0.10$ a.u., on the other hand, we found $\Delta E(f) = -0.0263$ a.u. and an eigenvalue of $-0.098\,54$ a.u. This demonstrates that our method certainly allows the determination of $\Delta E(f)$ and eigenvalues on the 0.001-a.u. level.

The energy resolution of about 0.001 a.u. also indicates to what extent our numerical method can resolve the order of single-particle orbitals wherever these are nearly degenerate. Problems with ordering eigenvalues properly are without consequences for the stability of our numerical procedure as long as almost-degenerate orbitals are clearly inside or outside the occupied spectrum; in particular, as in this case, the ordering problems disappeared as soon as self-consistency was achieved. They do affect

our calculations, however, if these orbitals happen to be close to the Fermi energy ε_F, which is always the case at level crossings between the highest occupied and the lowest unoccupied orbital. In the vicinity of such level crossings, self-consistency could not be achieved. Fortunately, the capability of our method to order eigenvalues correctly is somewhat higher than the absolute energy resolution discussed above. Nevertheless, there are two regions of f, i.e., 5.25 a.u. $> f >$ 4.75 a.u. and 3.75 a.u. $> f >$ 2 a.u. (compare Fig. 3), where, due to level crossings, regular converged solutions could not be obtained. In this case we used two alternative procedures to resolve this difficulty.

The most obvious way out of this degeneracy problem is to restrict the individual orbitals which are used to construct the electronic density (16), i.e., to select one of the almost-degenerate orbitals as being occupied. This is completely equivalent to reducing the variational space offered by the basis (13) by one of the competing orbitals, i.e., to projecting out the subspace spanned by this orbital. Comparing the ground-state energies of all possibilities of including one of the competing orbitals in the occupied spectrum then allows one to determine the correct ground state. This method, however, has the disadvantage that the eigenvalue of the eliminated orbital cannot be determined self-consistently. Thus alternatively we simply mix the almost-degenerate orbitals when constructing the density, enforcing proper normalization,

$$n(\xi,\eta) = \sum_{m=0}^{\infty}\sum_{j=1}^{\infty} \nu_{m,j} \left|\Psi_{j,m}(\xi,\eta)\right|^2 \quad ,$$

where $\nu_{m,j}$ equals ν_m, Eq. (17), for all inner orbitals, ν_m/M for the M competing orbitals at the Fermi surface and 0 otherwise. This leads to a stable series of eigenvalues near the Fermi surface at the price of not being consistent with the basic principles of DFT, as the ground state is no longer constructed from a single determinant. Consequently this method does not produce ground state energies [and consequently $\Delta E(f)$] in a consistent way (in contrast to the former approach involving only single-determinant wave functions). Thus the projection method has been used for the relevant critical f in Figs. 1 and 2. In order to get a complete picture of the Kohn-Sham eigenvalues, on the other hand, one has to apply the mixing procedure. Thus this scheme has been used for producing Fig. 3. It is important to note, however, that the most interesting quantity, $\Delta E(f)$, does not depend sensitively on the way the degeneracy situations are treated. Both procedures discussed lead to the same $\Delta E(f)$ within the accuracy that is required for this quantity.

It is instructive to consider $f = 5$ a.u. as an example for this situation. Here the first orbital with $m = 3$, $\Psi_{j=1,m=3}$, is almost degenerate with two other orbitals, $\Psi_{j=7,m=0}$ and $\Psi_{j=4,m=1}$, while six electrons (note the m and spin degeneracy) have to be distributed among these orbitals. Analyzing this case in detail shows that $\Psi_{j=7,m=0}$ is bound, while the right order of $\Psi_{j=1,m=3}$ and $\Psi_{j=4,m=1}$ cannot be resolved. Selecting $\Psi_{j=1,m=3}$ to be bound as discussed above leads to a ground-state energy $E_{\text{tot}} = -2.631\,43$ a.u.; using $\Psi_{j=4,m=1}$, one ends up with $E_{\text{tot}} = -2.631\,06$ a.u. The difference of 0.000 37 a.u. between both energies certainly is very close to (if

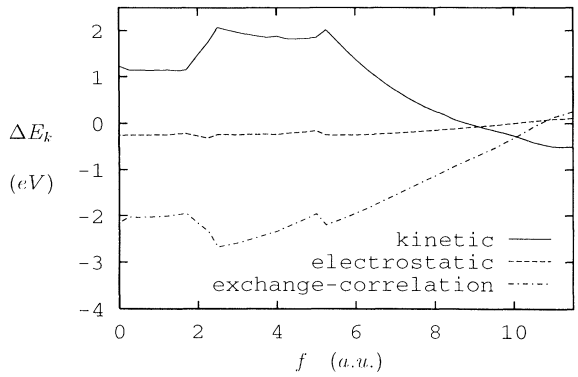

FIG. 2. Components of $\Delta E(f)$ for VWN (in eV): Kinetic energy (solid line), electrostatic energy (dashed line), and exchange-correlation energy (dashed-dotted line).

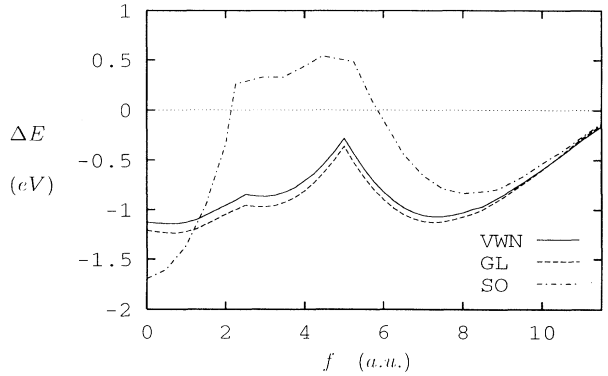

FIG. 1. $\Delta E(f)$, Eq. (1) (in eV) obtained using VWN (solid line) and GL (dashed line) in comparison to SO (dashed-dotted line).

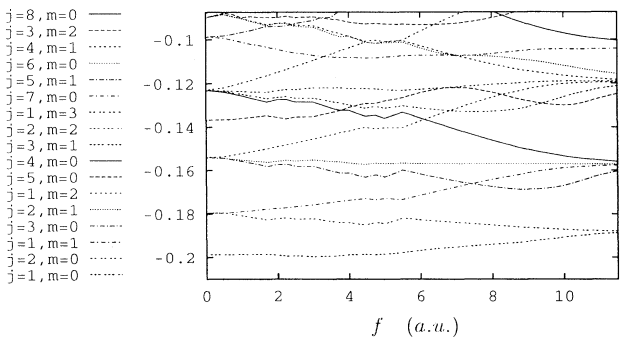

FIG. 3. Kohn-Sham eigenvalues (in a.u.) as a function of the cluster-cluster separation $f = d/2$ for VWN. The ordering of the counting number j corresponds to the united Na_{38} cluster.

not beyond) the limits of our method. The separation of the corresponding eigenvalues is extremely small: Using the mixing scheme one obtains $\epsilon_{70} = -0.101\,50$ a.u., $\epsilon_{41} = -0.100\,96$ a.u., and $\epsilon_{13} = -0.100\,88$ a.u. Of course, the absolute values of these eigenvalues should not be taken seriously beyond the 10^{-3}-a.u. level. Nevertheless, they most clearly indicate the degree of degeneracy present. This is, however, the most extreme case that has occurred. In contrast to $f = 5$ a.u., for all other values of f the ground state could be determined unambiguously.

IV. RESULTS

The main result of this work is given by Fig. 1, where we plot $\Delta E(f)$ as calculated using both the VWN and GL functionals in comparison to the results obtained by SO, which are based on the PZ functional (note that in Fig. 1 we use units of eV in order to spread the scale).

First, it is important to recognize that the qualitative behavior of $\Delta E(f)$ resulting from GL and VWN is very similar. In the interesting regime of cluster-cluster separations, $\Delta E(f)_{\mathrm{GL}}$ is more or less shifted by a constant value of roughly 0.1 eV with respect to $\Delta E(f)_{\mathrm{VWN}}$. The obvious tendency of the GL form to produce a somewhat stronger binding is in agreement with its electron-gas properties[30,31] (for a comparison of GL and VWN for the case of atomic dimers, see Ref. 39). Quantitatively the differences between GL, VWN, and PZ results for jellium sphere problems are most readily discussed for the spherically averaged unpolarized Na_{38} cluster. Using GL one obtains as ground-state energy $-2.863\,47$ a.u.; with VWN one finds $-2.662\,62$ a.u., while PZ gives $-2.671\,90$ a.u. As to be expected, VWN and PZ results agree very well, as these functionals are based on the same numerical correlation energy results.[35] The difference between the GL and VWN results is similar for the smaller Na_{19} system (GL: $-1.409\,50$ a.u., VWN: $-1.310\,60$ a.u., PZ: $-1.314\,76$ a.u.). It is this 7% difference in ground-state energies which produces the shift between $\Delta E(f)_{\mathrm{GL}}$ and $\Delta E(f)_{\mathrm{VWN}}$. In the present context, however, this shift is not relevant: The stability of $(Na_{19})_2$ dimers only depends on the height and width of the barrier between the local minimum at $f = 7.5$ a.u. and the absolute minimum at $f = 0.75$ a.u., but the structure of the barrier is very similar for both functionals. Nevertheless, one conclusion to be drawn from these results is that binding energies and eigenvalues of jellium model calculations depend appreciably on the $E_{\mathrm{xc}}[n]$ used in Kohn-Sham equations. It certainly seems recommendable to use one of the more accurate forms for $E_{\mathrm{xc}}^{\mathrm{LDA}}[n]$.[30,31,40]

The differences between the VWN results and those of SO, on the other hand, are more dramatic. While the location of the local minimum of $\Delta E(f)$ is about the same (8 a.u. for SO compared to 7.5 a.u. in our case), its depth differs by about 0.3 eV, with our ΔE being more attractive. The opposite happens for the united Na_{38} cluster. Here we find $\Delta E(f = 0) = -1.127$ eV (using a spherical average for the open $2p$ shell — this procedure might lead to a marginally higher ground-state energy than taking into account the nonsphericity of the electronic density), in comparison to -1.7 eV of SO. Note that while our $\Delta E(f = 0)$ results from the solution of one-center Kohn-Sham equations for a spherical Na_{38} cluster (and thus from a completely different numerical program), SO obtain their united cluster energy using $f = 10^{-4}$ a.u., i.e., on the basis of the two-center code used for other f. The fact that the results from our two-center code run rather smoothly into the united cluster energy obtained from a much simpler and more accurate one-center program strongly supports the accuracy of our two-center calculations. Furthermore, in contrast to the results of SO, our $\Delta E(f)$ for small f indicates that our method is able to reproduce rather subtle energy differences, as the spherically averaged Na_{38} leads to a higher ground-state energy than a Na_{38} cluster with a small deformation (the smallest f for which we carried through a calculation with the two-center code is 0.25 a.u.), in accordance with previous results.[13] For large values of f, which are easier to deal with from a computational point of view, our $\Delta E(f)$ becomes identical with that of SO, as one would expect from the similarity of VWN and PZ results for unpolarized systems.

More important than the limiting behavior of $\Delta E(f)$ for large and small f, however, are the differences in the structure and size of the barrier that separates the dimer minimum from the united cluster. Our barrier is produced by $\Psi_{j=1,m=3}$ entering the occupied orbitals. As soon as $\Psi_{j=1,m=3}$ is occupied, $\Delta E(f)$ starts to become more attractive again. The same happens at $f = 2.5$ a.u., where a new $m = 1$ orbital starts to be occupied, as can be seen from Fig. 3. Also, our barrier has a maximum of only -0.27 eV at $f = 5$ a.u. (corresponding to a height of 0.79 eV with respect to the dimer minimum at $f = 7.5$ a.u.—see Fig. 1). Consequently, the stability of the dimer configuration $(Na_{19})_2$ is substantially reduced as compared to the results of SO.

In Fig. 2 we show the individual contributions to $\Delta E(f)$ for the case of VWN. Again the f dependence is quite different from that of SO (compare Fig. 2 of Ref. 23). The individual terms of the binding energy show a somewhat smoother variation in our case.

Figure 3 shows the Kohn-Sham eigenvalues in the interesting regime of f, again for the VWN functional. One clearly recognizes how the shells of the spherical Na_{38} cluster develop into those of two spherical Na_{19} clusters. In particular, one notes how the lowest $m = 3$ orbital enters the occupied spectrum at about $f = 5$ a.u., finally joining the $1f$ shell of Na_{38}. It is this rearrangement of orbitals at the Fermi surface that is responsible for the increase of $\Delta E(f)$ at $f = 5$ a.u. As with $\Psi_{j=1,m=3}$, a new symmetry structure is introduced into the ground state; the peak of $\Delta E(f)$ at $f = 5$ a.u. is much more pronounced than the corresponding one at $f = 2.5$ a.u., where a different $m = 1$ orbital starts to be occupied.

Examining Fig. 3 in detail, one observes the two regions where the degeneracy of orbitals leads to convergence problems for pure single-determinant ground states (compare the comments in Sec. III). While for 4.75 a.u. $< f <$ 5.25 a.u., $\Psi_{j=7,m=0}$, $\Psi_{j=4,m=1}$, and $\Psi_{j=1,m=3}$ are more or less degenerate, the second critical region is due to an extended level crossing centered at $f = 2.5$ a.u. In

particular, for the more sensitive regime $4.5 < f < 5.25$, small discontinuities of the eigenvalues at the boundaries of this region reveal the fact that in this regime the almost-degenerate orbitals at the Fermi level have been mixed. Nevertheless, the overall smoothness of the eigenvalues in these critical regions clearly supports the method used to obtain them.

Figure 3 also shows that in the f regime of the dimer minumum (around $f = 7.5$ a.u.), one finds a substantial gap between the eigenvalues of the highest occupied ($\Psi_{j=7,m=0}$) and the lowest unoccupied ($\Psi_{j=3,m=2}$) orbital. Although in the framework of DFT only the eigenvalue of the highest occupied orbital has a rigorous physical meaning, i.e., it equals the ionization potential, this eigenvalue difference has been used in the literature as a measure for the reactivity of clusters. In this respect the comparably large gap at the dimer minimum indicates a low reactivity of the dimer. Note, however, that LDA eigenvalues for highest occupied orbitals can be in error by as much as 50% (compare Ref. 41).

V. CONCLUSIONS

In this contribution we have reconsidered the problem of metal cluster dimers for the case of $(Na_{19})_2$. On the basis of the jellium model, we have solved the two-center Kohn-Sham equations (using the LDA for exchange and correlation) for a geometry proposed in the literature.[23] We find that the barrier that separates the minimum in binding energy defining the cluster dimer from the absolute energy minimum corresponding to the united cluster is considerably smaller than previously reported.[23] Thus the transition of the dimer to the united Na_{38} cluster is more likely on the basis of our results. In addition, the attractive force between two well separated Na_{19} clusters is even stronger in our case, i.e., the dimer minimum is deeper. Consequently, the mechanism for fusion of two Na_{19} clusters via the dimer channel, as put forward in Ref. 23, is confirmed by our results and thus could be the explanation for the relatively high abundance of the nonmagic Na_{38} cluster observed in experiments.[24]

Our calculations indicate that Na_{38} is a deformed system: For the jellium geometry considered in this work, a separation of about 1.5 a.u. between the two centers leads to a lower ground-state energy than a spherical cluster. Though this geometry most likely does not represent the most suitable form for the jellium background, and the spherical average used for the electronic density in the case of the spherical jellium might lead to a marginally higher energy than treating the open $2p$ shell nonspherically, this fact reflects the deformation of Na_{38} found in previous studies.[13]

Furthermore, we present a correlation diagram obtained from the self-consistent solution of Kohn-Sham equations for two-center cluster problems. This result should provide some insight into the various possibilities of electron excitations and transfer in low-energy cluster-cluster collisions. Work along this line is in progress.

ACKNOWLEDGMENTS

We would like to thank the Institut für Angewandte und Instrumentelle Mathematik and the Hochschulrechenzentrum der Universität Frankfurt as well as the Gesellschaft für Schwerionenforschung (GSI), Darmstadt, for providing the computational power required for this work. Two of the authors (P.C. and O.K.) gratefully acknowledge financial support by the Heraeus Stiftung and the Alexander von Humboldt Stiftung, respectively. E.E., U.R.S., H.-J.L., A.T., E.W., and R.M.D. acknowledge support by the Deutsche Forschungsgemeinschaft.

APPENDIX: THE BACKGROUND POTENTIAL FOR OVERLAPPING JELLIUM SPHERES

For the calculation of $v_{\rm ext}(\mathbf{r})$ in the case of overlapping jellium spheres,

$$v_{\rm ext}(\mathbf{r}) = -\int d^3r' \frac{n_+(\mathbf{r}')}{|\mathbf{r}-\mathbf{r}'|} \quad , \tag{A1}$$

with $n_+(\mathbf{r})$ given by Eq. (3), we used spherical coordinates,

$$r = f\sqrt{\xi^2+\eta^2-1},$$
$$\cos\theta = \frac{\xi\eta}{\sqrt{\xi^2+\eta^2-1}} \quad ,$$

and a multipole expansion,

$$v_{\rm ext}(r,\theta) = \sum_{l=0}^{\infty}\left(a_l r^l + \frac{b_l}{r^{l+1}}\right)P_l(\cos\theta) \quad . \tag{A2}$$

The potential (A1) can be directly evaluated along the z axis,

$$v_{\rm ext}(r,0) = -2\pi n_0\Big\{ \frac{2}{3}\frac{f}{r^2-f^2}(r^2+R_d^2-f^2)^{\frac{3}{2}} - \frac{1}{3}\frac{1}{r-f}|r-R_d-f|^3 + \frac{1}{3}\frac{1}{r+f}|r+R_d+f|^3$$
$$-2(R_d+f)r\Theta(r-R_d-f) - [(R_d+f)^2+r^2]\Theta(R_d+f-r)\Big\} \quad . \tag{A3}$$

Equation (A3) allows the determination of the coefficients a_l, b_l of Eq. (A2) by expansion in powers of either r or $1/r$. The two scales involved are given by f and $\sqrt{R_d^2-f^2}$. For $r < f$ and $r < \sqrt{R_d^2-f^2}$, one obtains a pure series in powers of r, as the numerator in (A3) can be expanded in powers of $r/\sqrt{R_d^2-f^2}$ and the denominators in powers of r/f. The opposite situation, $r > f, r > \sqrt{R_d^2-f^2}$, requires expansions in powers of f/r and $\sqrt{R_d^2-f^2}/r$ and consequently all a_l vanish. In the intermediate regime one has to distinguish two cases

depending on the relative size of f and $\sqrt{R_d^2 - f^2}$, and thus both a_l and b_l contribute. Of course, only even multipoles are relevant for all these expansions in the case of the symmetric $(Na_{19})_2$ dimer.

In our calculations we used the multipole expansion (A2) to obtain v_{ext} with an accuracy of 10^{-8} a.u. with up to 4000 terms contributing. In particular, we made sure that none of the points of our Gaussian meshes was too close to the critical radius $r = f$, where the corresponding expansions do not converge.

[1] W. Ekardt, Phys. Rev. B **29**, 1558 (1984).
[2] D. E. Beck, Solid State Commun. **49**, 381 (1984).
[3] M. Y. Chou, A. Cleland, and M. L. Cohen, Solid State Commun. **52**, 645 (1984).
[4] W. A. de Heer, W. D. Knight, M. Y. Chou, and M. L. Cohen, Solid State Phys. **40**, 93 (1987).
[5] *Nuclear Physics Concepts in the Study of Atomic Cluster Physics*, edited by R. Schmidt, H. O. Lutz, and R. M. Dreizler, Lecture Notes in Physics Vol. 404 (Springer, Berlin, 1992).
[6] W. D. Knight, K. Clemenger, W. A. de Heer, W. A. Saunders, M. Y. Chou, and M. L. Cohen, Phys. Rev. Lett. **52**, 2141 (1984).
[7] M. Y. Chou and M. L. Cohen, Phys. Lett. **113A**, 420 (1986).
[8] J. Pedersen, S. Bjornholm, J. Borggreen, K. Hansen, T. P. Martin, and H. D. Rasmussen, Nature **353**, 733 (1991).
[9] T. P. Martin, S. Bjornholm, J. Borggreen, C. Bréchignac, Ph. Cahuzac, K. Hansen, and J. Pedersen, Chem. Phys. Lett. **186**, 53 (1991).
[10] T. P. Martin, T. Bergmann, H. Göhlich, and T. Lange, J. Phys. Chem. **95**, 6421 (1991); Z. Phys. D **19**, 25 (1991).
[11] O. Genzken and M. Brack, Phys. Rev. Lett. **67**, 3286 (1991).
[12] K. Clemenger, Phys. Rev. B **32**, 1359 (1985).
[13] W. Ekardt and Z. Penzar, Phys. Rev. B **38**, 4273 (1988); Z. Peuzar and W. Ekardt, Z. Phys. D **19**, 109 (1991).
[14] A. Rubio, L. C. Balbás, and J. A. Alonso, Z. Phys. D **19**, 93 (1991).
[15] W. Ekardt, Phys. Rev. Lett. **52**, 1925 (1984).
[16] W. Ekardt, Phys. Rev. B **31**, 6360 (1985).
[17] W. Ekardt, Phys. Rev. B **32**, 1961 (1985).
[18] G. Bertsch and W. Ekardt, Phys. Rev. B **32**, 7659 (1985).
[19] M. J. Puska, R. M. Nieminen, and M. Manninen, Phys. Rev. B **31**, 3486 (1985).
[20] D. E. Beck, Phys. Rev. B **35**, 7325 (1987).
[21] W. Ekardt and Z. Penzar, Phys. Rev. B **43**, 1322 (1991).
[22] B. Wassermann and W. Ekardt, Z. Phys. D **19**, 97 (1991).
[23] S. Saito and S. Ohnishi, Phys. Rev. Lett. **59**, 190 (1987); in *Physics and Chemistry of Small Clusters*, edited by P. Jena, B. K. Rao, and S. N. Khanna (Plenum, New York, 1987), p. 115.
[24] W. D. Knight, W. A. de Heer, K. Clemenger, and W. A. Saunders, Solid State Commun. **53**, 445 (1985).
[25] Y. Ishii, S. Saito, and S. Ohnishi, Z. Phys. D **7**, 289 (1987).
[26] S. Saito and M. L. Cohen, Phys. Rev. B **38**, 1123 (1988).
[27] M. Nakamura, Y. Ishii, A. Tamura, and S. Sugano, Z. Phys. D **19**, 145 (1991).
[28] R. Schmidt, G. Seifert, and H. O. Lutz, Phys. Lett. A **158**, 231 (1991); G. Seifert, R. Schmidt, and H. O. Lutz, *ibid.* **158**, 237 (1991).
[29] O. Gunnarsson and B. I. Lundqvist, Phys. Rev. B **13**, 4274 (1976).
[30] S. H. Vosko, L. Wilk, and M. Nusair, Can. J. Phys. **58**, 1200 (1980).
[31] J. P. Perdew and A. Zunger, Phys. Rev. B **23**, 5048 (1981).
[32] J. Eichler and U. Wille, Phys. Rev. A **11**, 1973 (1975).
[33] A. Toepfer, E. K. U. Gross, and R. M. Dreizler, Phys. Rev. A **20**, 1808 (1979); Z. Phys. A **298**, 167 (1980).
[34] R. M. Dreizler and E. K. U. Gross, *Density Functional Theory* (Springer, Berlin, 1990).
[35] D. M. Ceperley and B. J. Alder, Phys. Rev. Lett. **45**, 566 (1980).
[36] E. A. Hylleraas, Z. Phys. **71**, 739 (1931).
[37] *Handbook of Mathematical Functions*, edited by M. Abramowitz and I. A. Stegun (Dover, New York, 1965).
[38] B. C. Carlson and G. L. Morley, Am. J. Phys. **31**, 209 (1963).
[39] G. S. Painter, Phys. Rev. B **24**, 4264 (1981); G. S. Painter and F. W. Averill, *ibid.* **26**, 1781 (1982); R. O. Jones, J. Chem. Phys. **76**, 3098 (1982).
[40] J. P. Perdew, in *Electronic Structure of Solids 1991*, edited by P. Ziesche and H. Eschrig (Akademie Verlag, Berlin, 1991), Vol. 11.
[41] E. Engel and S. H. Vosko, Phys. Rev. A **47**, 2800 (1993).